

Monitoring statistics of the ERS-2 scatterometer for ESA cycle 107

(Project Ref. 18212/04/I-OL)

Hans Hersbach

European Centre for Medium-Range Weather Forecasts,

Shinfield Park, Reading, RG2 9AX, England

Tel: (+44 118) 9499476, e-mail: dal@ecmwf.int

August 24, 2005

1 Introduction

The quality of the UWI product was monitored at ECMWF for cycle 107. Results were compared to those obtained from the previous cycle, as well for data received during the nominal period in 2000 (up to cycle 59). No corrections for duplicate observations were applied.

During cycle 107 data was received between 21:06 UTC 11 July 2005 and 13:48 UTC 15 August 2005. No data was received for the 6-hourly batches between 18 UTC 12 August and 18 UTC 13 August 2005, for 06 UTC 14 August 2005 and for 18 UTC 15 August 2005.

Data is being recorded whenever within the visibility range of a ground station. For cycle 107 data coverage was over the North-Atlantic, part of the Mediterranean, the Caribbean, the Gulf of Mexico, a small part of the Pacific west from the US Canada and Central America, the Chinese and Japanese Sea, and the Southern Ocean south of Australia and New Zealand (see Figure 2).

The asymmetry between the fore and aft incidence angles showed many peaks, mostly behaving within reasonable bounds. The k_p -yaw ESA flag was set accordingly.

Compared to cycle 106, the UWI wind speed relative to ECMWF first-guess (FG) fields showed a slightly increased standard deviation (from 1.29 to 1.33 m/s), announcing the onset of an up-going trend as also observed one year ago. In agreement with that trend the large relative bias of the UWI wind speed slightly decreased from -1.02 to -0.98 m/s. The trend of low standard deviation in summer is clearly the result of a milder wind climate (mainly Northern-Hemispheric data coverage).

The yearly cycle of the large negative bias is less obviously connected to seasonal effects in the sampled region. However, statistics for QuikSCAT winds limited to the main area of ERS-2 data coverage (Figure 17) now do confirm this relation.

The performance of the UWI wind direction degraded somewhat near the end cycle 107. The quality of the with ECMWF FG winds de-aliased wind direction was stable, however. This indicates some problems in the UWI de-aliasing software (which does not make use of these model winds).

Ocean calibration was stable, showing a large inter-node and inter-beam dependency of bias levels. The average bias level remained quite negative (-0.92 dB, was -0.91 dB), especially at high incidence angles (Figure 4).

Data originating from the recently included stations in Beijing and McMurdo (Antarctica, see previous cyclic report) compared well with ECMWF model winds.

The ECMWF assimilation/forecast system was not changed during cycle 107.

The cycle-averaged evolution of performance relative to ECMWF first-guess (FG) winds is displayed in Figure 1. Figure 2 shows global maps of the over cycle 107 averaged UWI data coverage and wind climate, Figure 3 for performance relative to FG winds.

2 ERS-2 statistics from 12 July to 15 August 2005

2.1 Sigma0 bias levels

The average sigma0 bias levels (compared to simulated sigma0's based on ECMWF model FG winds) stratified with respect to antenna beam, ascending or descending track and as function of incidence angle (i.e. across-node number) is displayed in Figure 4.

Inter-node and inter-beam (mainly mid versus the fore/aft beam) dependencies are like for cycle 106, still rather large. Bias levels of the fore and aft beam are the most negative ones, especially at high incidence angles. Average bias level is stable (-0.92 dB, was -0.91 dB), being 0.2 dB more negative than for nominal data in 2000 (see Figure 1 of the reports for cycle 48 to 59). The situation is similar to that of one year ago (see report for cycle 97), where large negative biases in both wind and backscatter were observed.

The data volume of descending tracks was about 15% lower than for ascending tracks.

2.2 Incidence angles

For ESACA, across-node binning is, like the old processor, retained on a 25km mesh. From simple geometrical arguments it follows that variations in yaw attitude will lead to asymmetries between the incidence angles of the fore and aft beam. Indeed, this has been observed. Figure 5 gives a time evolution of this asymmetry, showing rapid variations, which are typical for yaw attitude errors. Also in this Figure, the occasions for which the combined k_p -yaw quality flag was set are indicated by red

stars. The relation with incidence-angle asymmetries is obvious.

During cycle 107 most peaks were within bounds.

2.3 Distance to cone history

The distance to the cone history is shown in Figure 6. Curves are based on data that passed all QC, including the test on the k_p -yaw flag, and subject to the land and sea-ice check at ECMWF (see cyclic report 88 for details).

Like for cycle 106, time series are (due to lack of statistics) very noisy, especially for the near-range nodes. Most spikes were found to be the result of low data volumes.

Compared to cycle 106, the average level was slightly higher (from 1.22 to 1.23), and is now about 13% higher than for nominal data (see top panel Figure 1).

2.4 UWI minus First-Guess wind history

In Figure 7, the UWI minus ECMWF first-guess wind-speed history is plotted.

The history plot shows several peaks, most of which are related to low data volumes. Similar results apply for the history of de-aliased CMOD4 winds versus FG (Figure 9).

Figure 11 displays the locations for which UWI winds were more than 8 m/s weaker (top panel) and more than 8 m/s stronger (lower panel) than FG winds. Like for cycle 106, the number of such collocations is low. Two cases for stronger UWI winds are presented in Figure 12. The top panel shows the capture of Hurricane Emily on 16 July 2005, when it was around its maximal strength (Category 4). CMOD5-inverted winds up to 65 knots were actively assimilated at ECMWF. Maximal winds were increased from 18.0 m/s in the first guess to 21.2 m/s in the analysis, although, the scatterometer data was not able to move the misplaced model vortex to the correct location.

The lower panel of Figure 12 shows Typhoon Matsa, being observed on 4 August 2005 by ERS-2 scatterometer data that was processed by the recently included station in Beijing. Also this data was well-assimilated at ECMWF, and maximal model winds increased from 19.8 m/s to 21.3 m/s (for more information, see also www.esa.int/esaEO/SEM89U808BE.index_0.html).

Average bias levels and standard deviations of UWI winds relative to FG winds are displayed in Table 1. From this it is seen that the bias of both the UWI and CMOD4 product have become slightly less negative. The average bias level is lower to that for nominal data in 2000 (UWI: -0.99 m/s now, was -0.79 m/s for cycle 59).

The trend of the large increase of negative bias between April and July, and the onset to smaller values in August was also observed during 2004. It was not clear whether this yearly cycle was a result of (seasonally dependent) drifts in the AMI instrument, or whether it is a result from seasonally dependent geophysical conditions in the mainly Northern Hemispheric coverage. In previous cyclic reports it was shown that there was a similar (though much smaller) signal in the globally averaged bias evolution of QuikSCAT. Such statistics have now been limited to an

	cycle 106		cycle 107	
	UWI	CMOD4	UWI	CMOD4
speed STDV	1.29	1.29	1.33	1.33
node 1-2	1.35	1.35	1.39	1.38
node 3-4	1.30	1.30	1.35	1.34
node 5-7	1.25	1.26	1.31	1.31
node 8-10	1.25	1.26	1.27	1.28
node 11-14	1.24	1.25	1.29	1.29
node 15-19	1.28	1.28	1.31	1.32
speed BIAS	-1.02	-1.02	-0.98	-0.99
node 1-2	-1.40	-1.39	-1.38	-1.37
node 3-4	-1.21	-1.18	-1.19	-1.16
node 5-7	-1.04	-1.02	-1.01	-0.99
node 8-10	-0.91	-0.91	-0.87	-0.87
node 11-14	-0.87	-0.89	-0.83	-0.86
node 15-19	-0.89	-0.92	-0.85	-0.90
direction STDV	27.2	18.4	28.8	18.7
direction BIAS	-3.3	-3.7	-3.3	-3.5

Table 1: Biases and standard deviation of ERS-2 versus ECMWF FG winds in m/s for speed and degrees for direction.

area well-covered by ERS-2: (20N-90N, 80W-20E), including the Northern Atlantic, the North Sea and the Mediterranean. In Figure 17 time series are shown for this area for both ERS-2 (top panel) and QuikSCAT (lower panel) for the period between 1 January 2004 and the 15 August 2005 (end of cycle 107). Results are shown for at ECMWF actively assimilated data, i.e., CMOD5 winds for ERS-2 and 4% reduced QuikSCAT winds on a 50km resolution. This Figure clearly shows that a very similar seasonal trend exists for QuikSCAT, i.e., the yearly variations are likely to be induced by seasonally changing geophysical conditions, creating location and seasonal dependent biases between ECMWF 10-metre winds and scatterometer backscatter. Inspection of bias maps of QuikSCAT and ERS-2 shows that part of the negative bias in summer is related to a more frequent stable atmospheric density stratification than in winter time.

The standard deviation of UWI wind speed compared to cycle 106 has increased somewhat (1.33 m/s, was 1.29 m/s), the main reason being a less mild wind climate.

For cycle 107 the (UWI - FG) direction standard deviations were mostly ranging between 15 and 40 degrees (Figure 8). Sharp peaks are the result of low data volumes. From 6 August 2005 onwards, there was an increase. This transition was not observed in the time series of (de-aliased CMOD4 - FG) direction standard deviation (Figure 10), indication temporary problems in the UWI de-aliasing software.

Due to this trend, the average performance for UWI wind direction was slightly reduced (STDV 28.8 degrees, was 27.2 degrees, bias -3.3 degrees, unchanged), while that of de-aliased CMOD4 winds was more stable (18.7 degrees, was 18.4 degrees).

2.5 Scatterplots

Scatterplots of FG winds versus ERS-2 winds are displayed in Figures 13 to 16. Values of standard deviations and biases are slightly different from those displayed in Table 1. Reason for this is that, for plotting purposes, the in 0.5 m/s resolution ERS-2 winds have been slightly perturbed (increases scatter with 0.02 m/s), and that zero wind-speed ERS-2 winds have been excluded (decreases scatter with about 0.05 m/s).

The scatterplot of UWI wind speed versus FG (Figure 13) is very similar to that for (at ECMWF inverted) de-aliased CMOD4 winds (Figure 15). It confirms that the ESACA inversion scheme is working properly.

Winds derived on the basis of CMOD5 are displayed in Figure 16. The relative standard deviation is lower than for CMOD4 winds (1.33 m/s versus 1.36 m/s). Compared to ECMWF FG, CMOD5 winds are -0.60 m/s slower; this average arising from mostly moderate winds. The agreement for the more extreme winds is very good.

Figure Captions

Figure 1: Evolution of the performance of the ERS-2 scatterometer averaged over 5-weekly cycles from 12 December 2001 (cycle 69) to 15 August 2005 (end cycle 107) for the UWI product (solid, star) and de-aliased winds based on CMOD4 (dashed, diamond). Results are based on data that passed the UWI QC flags. For cycle 85 two values are plotted; the first value for the global set, the second one for the regional set. Dotted lines represent values for cycle 59 (5 December 2000 to 17 January 2001), i.e. the last stable cycle of the nominal period. From top to bottom panel are shown the normalized distance to the cone (CMOD4 only) the standard deviation of the wind speed compared to FG winds, the corresponding bias (for UWI winds the extreme inter-node averages are shown as well), and the standard deviation of wind direction compared to FG.

Figure 2: Average number of observations per 12H and per 125km grid box (top panel) and wind-climate (lower panel) for UWI winds that passed the UWI flags QC and a check on the collocated ECMWF land and sea-ice mask.

Figure 3: The same as Figure 2, but now for the relative bias (top panel) and standard deviation (lower panel) with ECMWF first-guess winds.

Figure 4: Ratio of $< \sigma_0^{0.625} > / < \text{CMOD4}(\text{FirstGuess})^{0.625} >$ converted in dB for the fore beam (solid line), mid beam (dashed line) and aft beam (dotted line), as a function of incidence angle for descending and ascending tracks. The thin lines indicate the error bars on the estimated mean. First-guess winds are based on the in time closest (+3h, +6h, +9h, or +12h) T511 forecast field, and are bilinearly interpolated in space.

Figure 5: Time series of the difference in incidence angle between the fore and aft beam. Red stars indicate the occurrences for which the combined k_p -yaw flag was set.

Figure 6: Mean normalized distance to the cone computed every 6 hours for nodes 1-2, 3-4, 5-7, 8-10, 11-14 and 15-19). The dotted curve shows the number of incoming triplets in logarithmic scale (1 corresponds to 60,000 triplets) and the dashed one indicates the fraction of complete (based on the land and sea-ice mask at ECMWF) sea-located triplets rejected by ESA flags, or by the wind inversion algorithm (0: all data kept, 1: no data kept).

Figure 7: Mean (solid line) and standard deviation (dashed line) of the wind speed difference UWI - first guess for the data retained by the quality control.

Figure 8: Same as Fig. 7, but for the wind direction difference. Statistics are computed only for wind speeds higher than 4 m/s.

Figures 9 and 10: Same as Fig. 7 and 8 respectively, but for the de-aliased CMOD4 data.

Figure 11: Locations of data during cycle 107 for which UWI winds are more than 8 m/s weaker (top panel) respectively stronger (lower panel) than FG, and on which QC on UWI flags and the ECMWF land/sea-ice mask was applied.

Figure 12: Comparison between UWI (red) and ECMWF FG (blue) winds for hurricane Emily on 16 July 2005 (top panel) and Typhoon Matsa on 4 August 2005 (lower panel).

Figure 13: Two-dimensional histogram of first guess and UWI wind speeds, for the data kept by the UWI flags, and QC based on the ECMWF land and sea-ice mask. Circles denote the mean values in the y-direction, and squares those in the x-direction.

Figure 14: Same as Fig. 13, but for wind direction. Only wind speeds higher than 4m/s are taken into account.

Figure 15: Same as Fig. 13, but for de-aliased CMOD4 winds.

Figure 16: Same as Fig. 13, but for de-aliased CMOD5 winds.

Figure 17: Bias relative to FG winds of the wind speed of actively assimilated ERS-2 winds (based on CMOD5) for nodes 1-19 (top panel) respectively 50-km QuikSCAT (based on the QSCAT-1 model function and reduced by 4%) for nodes 5-34 (i.e., inner-beam zone; middle and lower panels), averaged over the area (20N-90N, 80W-20E), and displayed for the period 01 January 2004 - 15 August 2005. Curves represent centred 15-day running means. Vertical dashed blue lines mark ECMWF model changes.

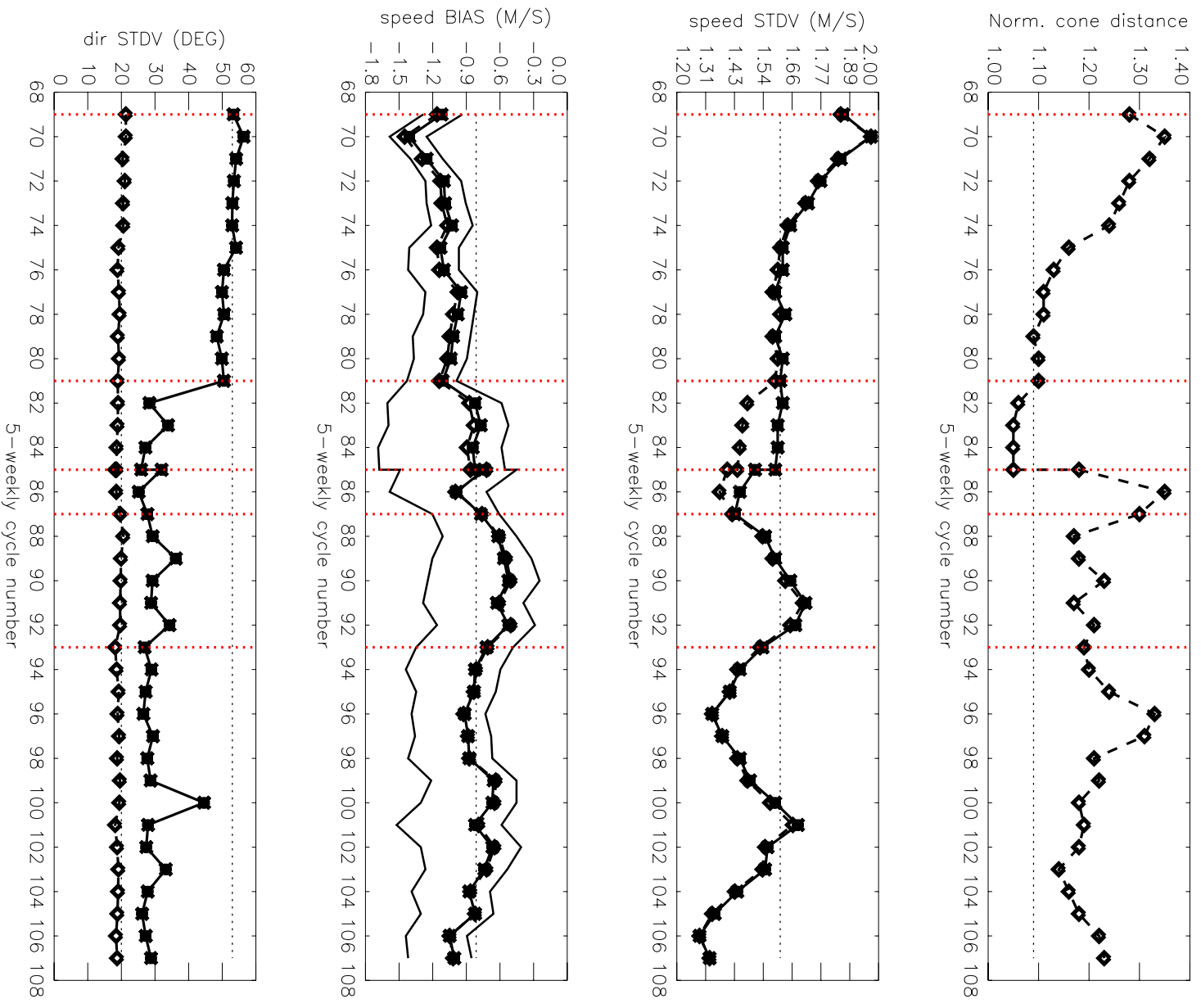
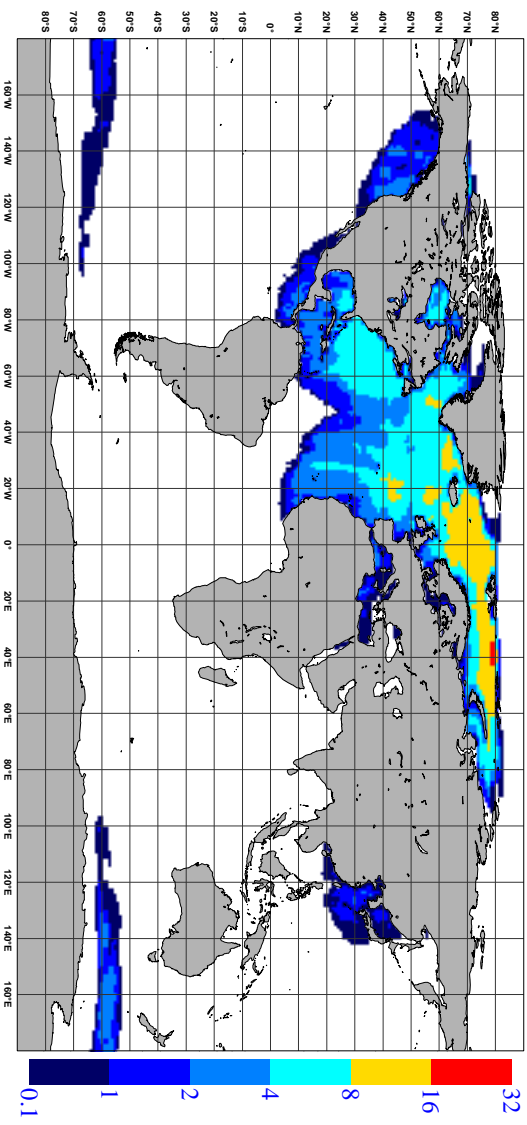


Figure 1

NOBS (ERS-2 UWI), per 12H, per 125km box
average from 2005071200 to 2005081518 GLOB:3.01



AVERAGE (ERS-2 UWI), in m/s.
average from 2005071200 to 2005081518 GLOB:5.56

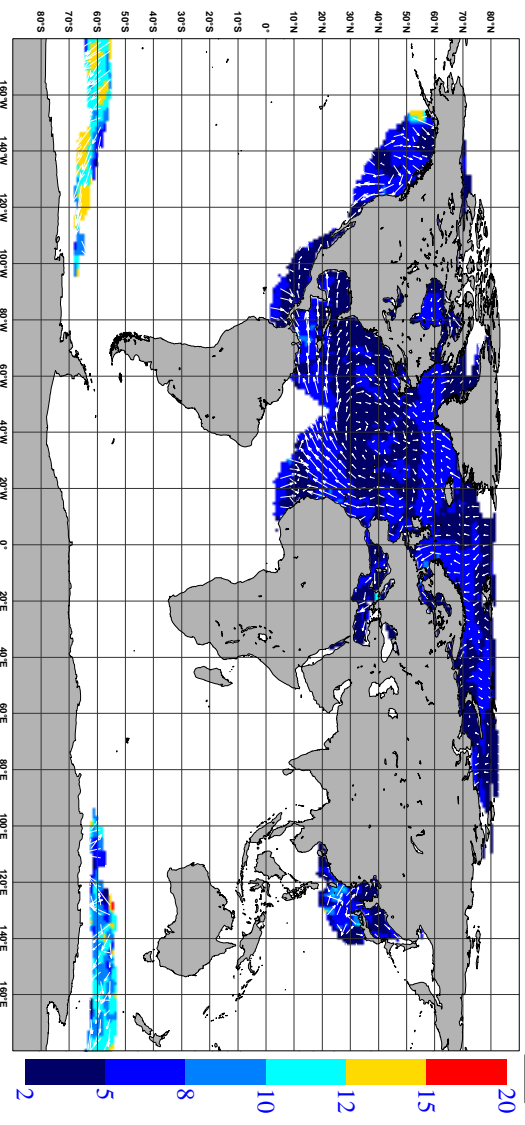
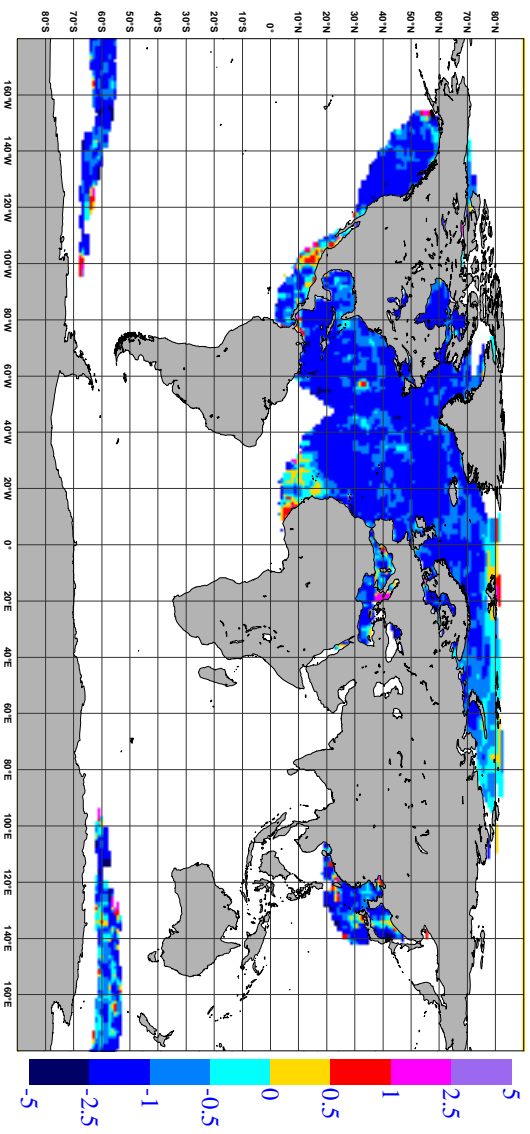


Figure 2

BIAS (ERS-2 UWI vs FIRST-GUESS), in m/s.
average from 2005071200 to 2005081518 GLOB:-1.09



STDV (ERS-2 UWI vs FIRST-GUESS), in m/s.
average from 2005071200 to 2005081518 GLOB:1.13

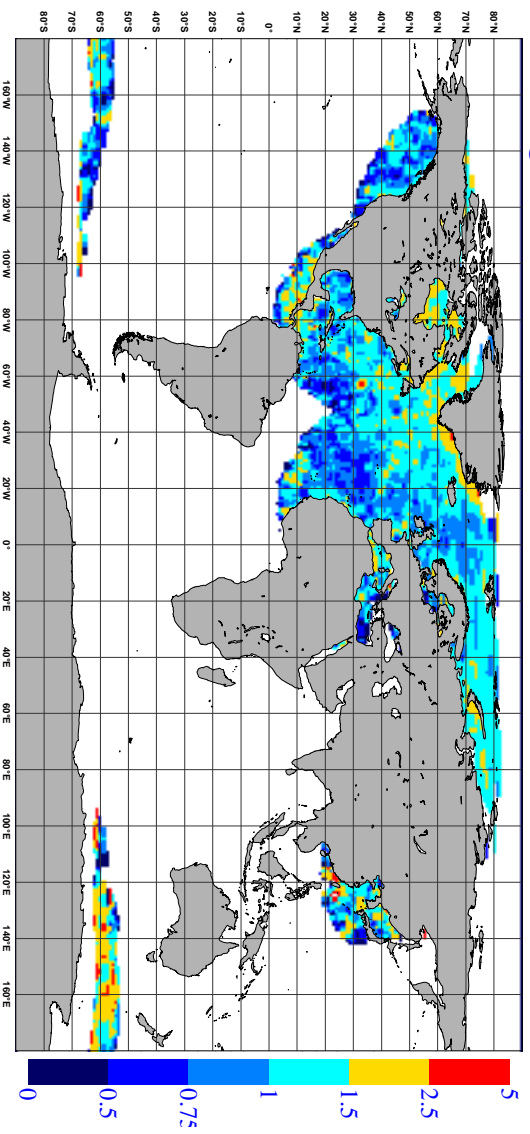


Figure 3

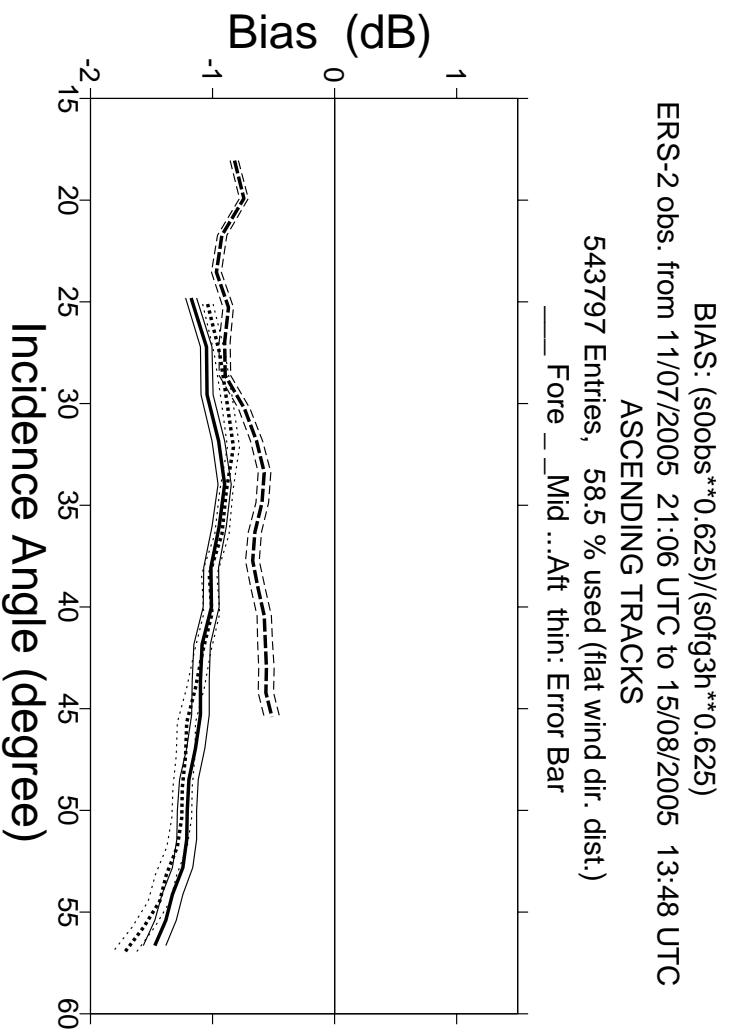
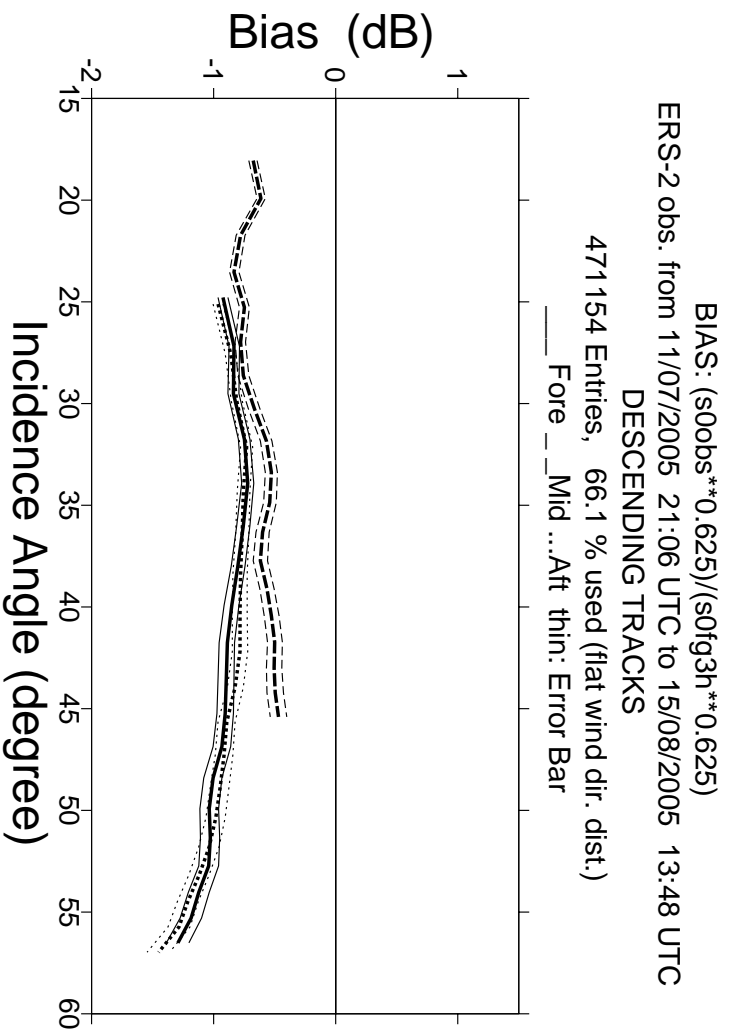


Figure 4

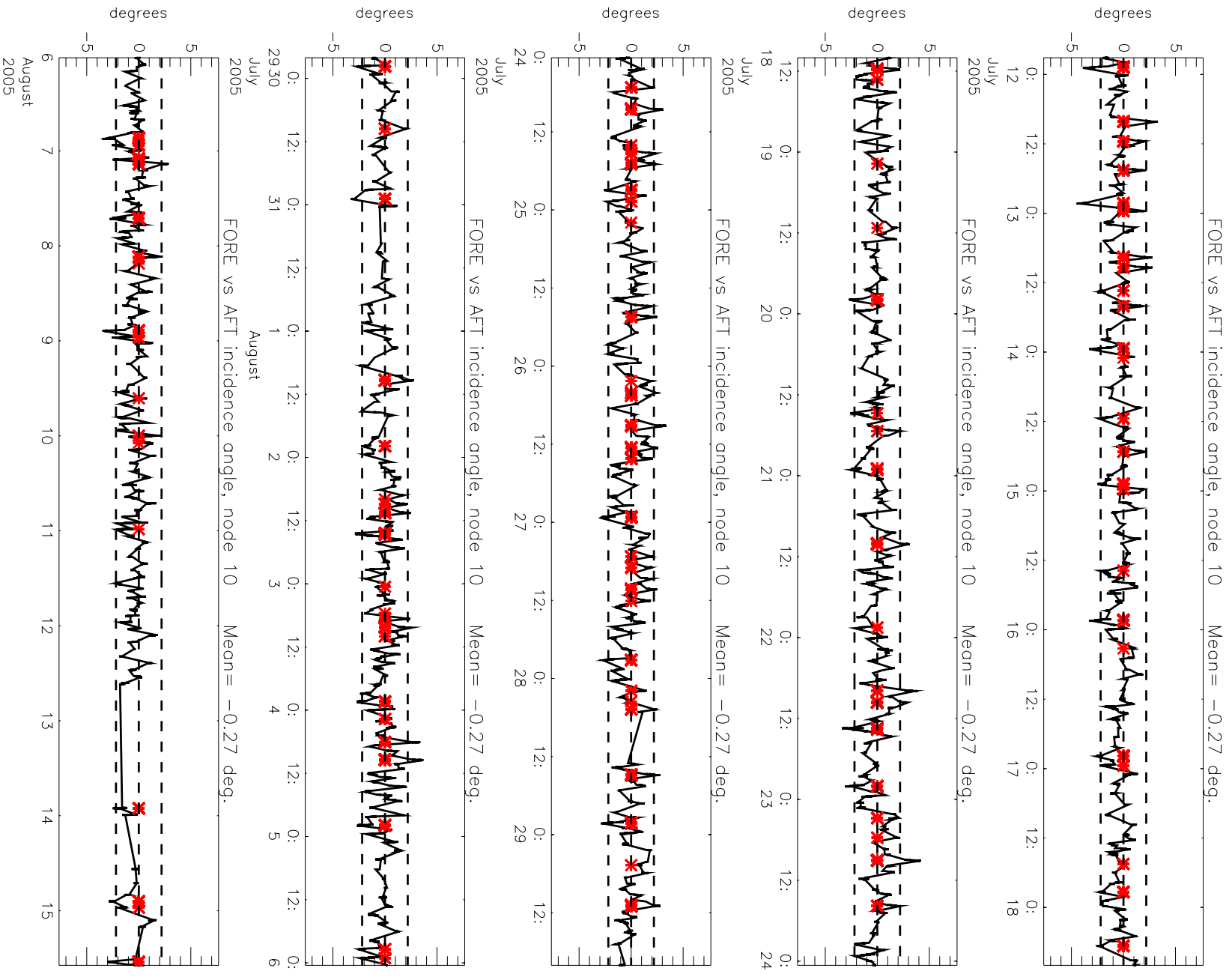


Figure 5

Monitoring of Sigma0 triplets versus CMOD4 for ERS-2

from 2005071200 to 2005081518

(solid) mean normalised distance to the cone over 6 h

(dashed) fraction of complete sea-point observations rejected by ESA flag or CMOD4 inversion

(dotted) total number of data in log. scale (1 for 60000)

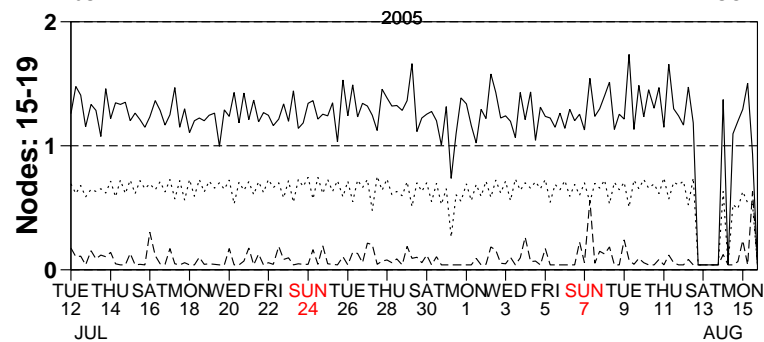
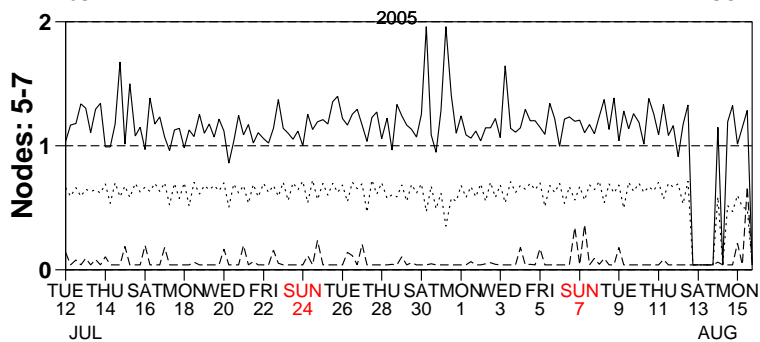
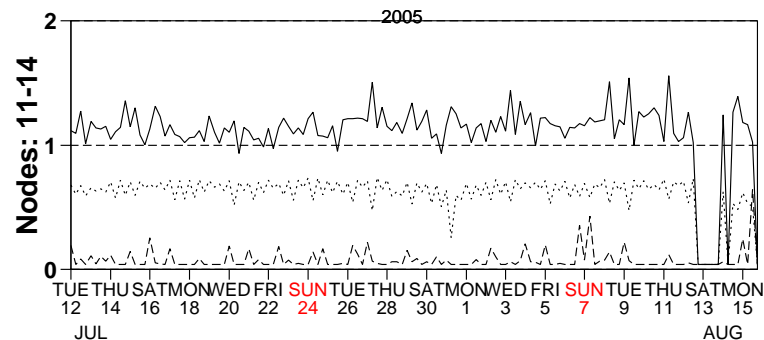
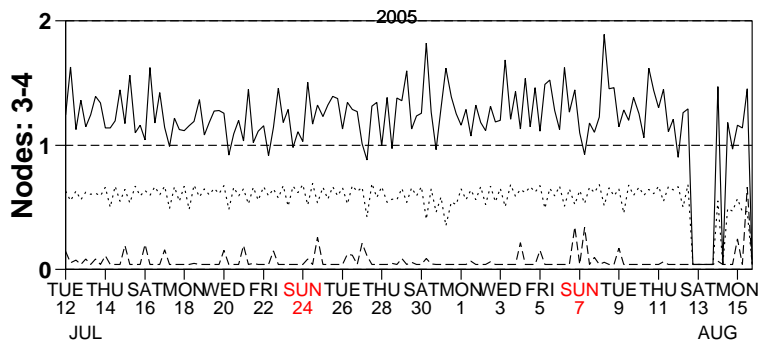
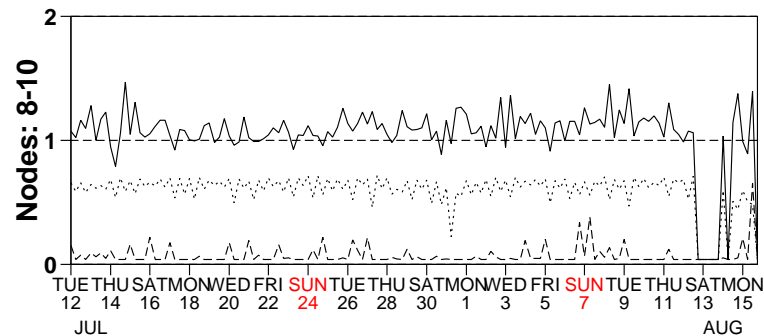
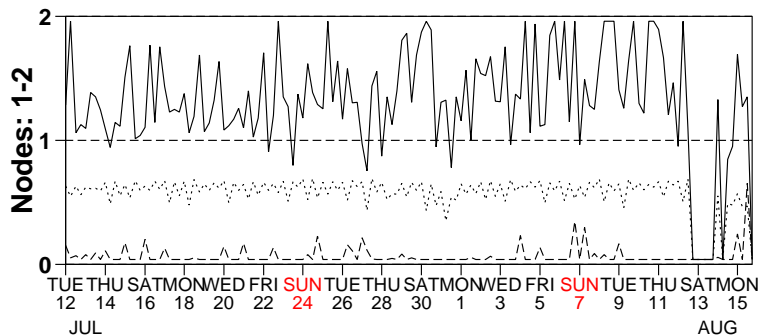


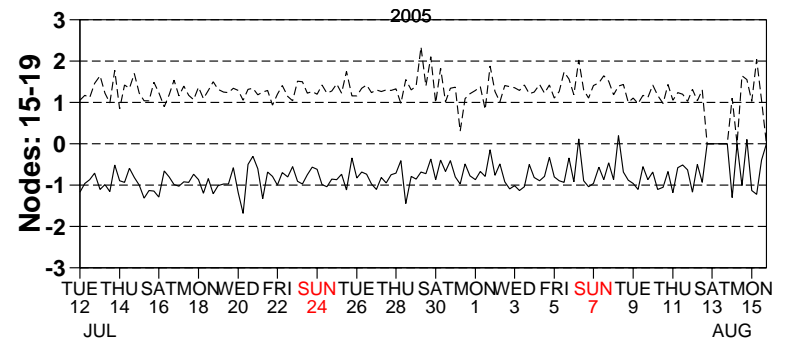
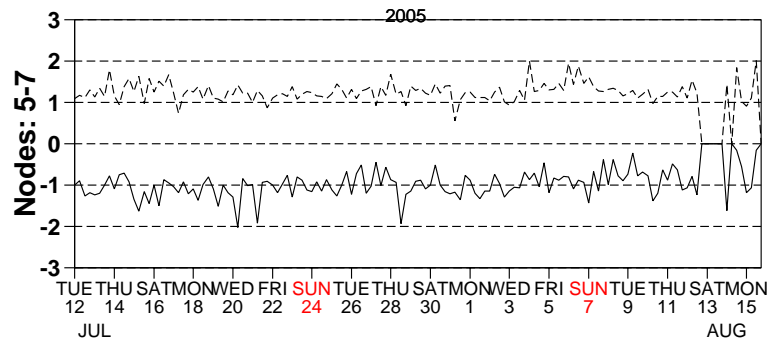
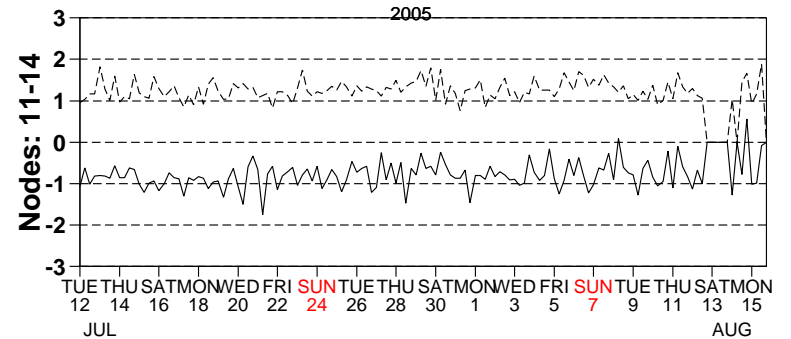
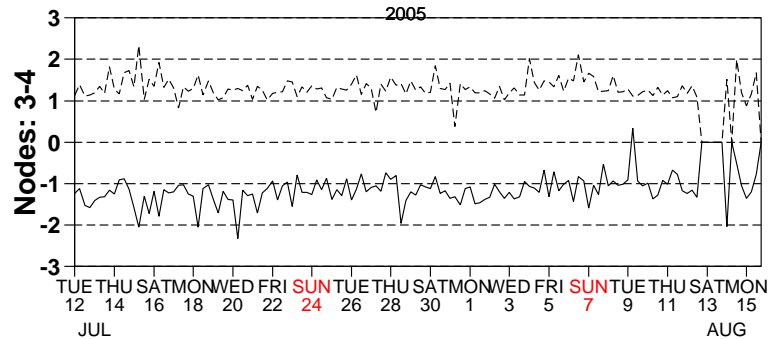
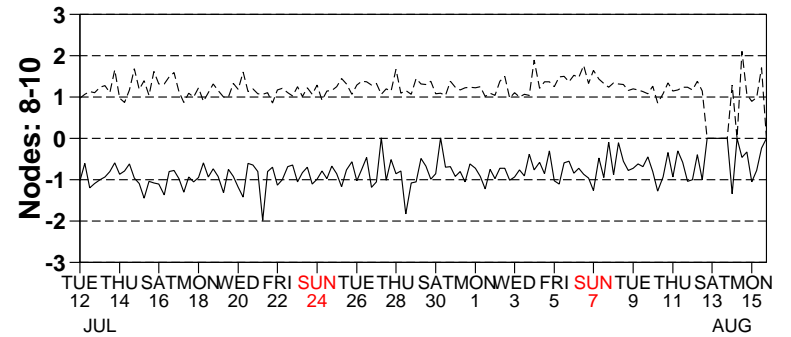
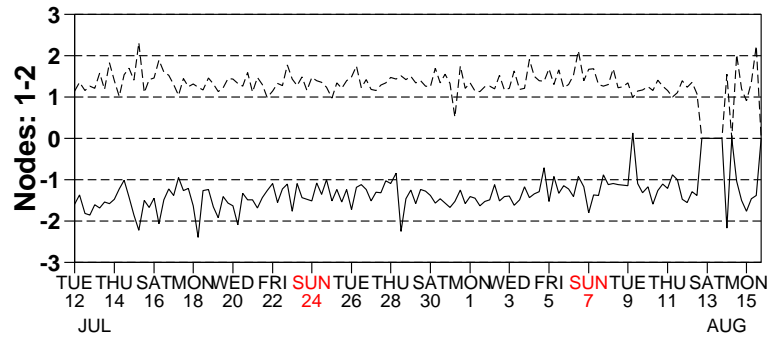
Figure 6

Monitoring of UWI winds versus First Guess for ERS-2

from 2005071200 to 2005081518

(solid) wind speed bias UWI - First Guess over 6h (deg.)

(dashed) wind speed standard deviation UWI - First Guess over 6h (deg.)



2005

2005

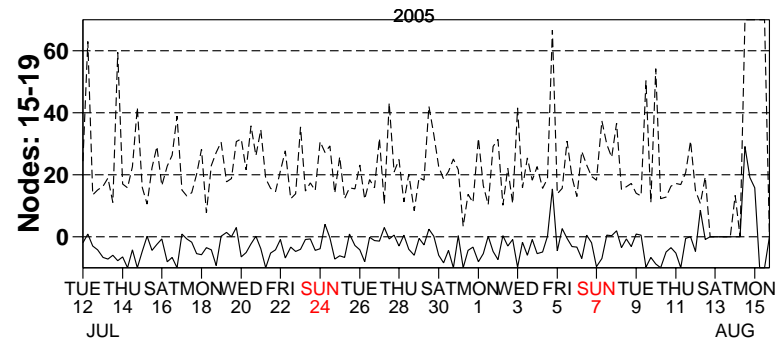
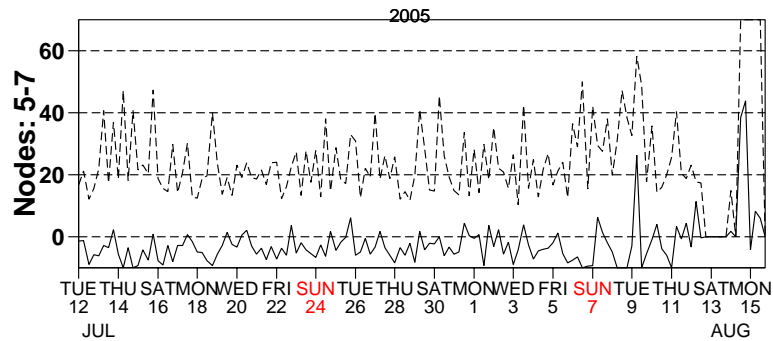
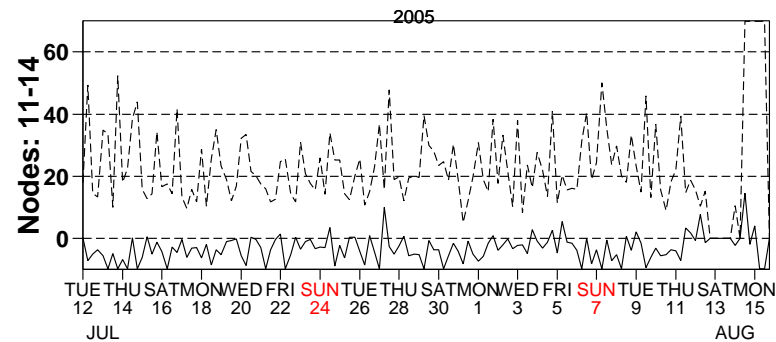
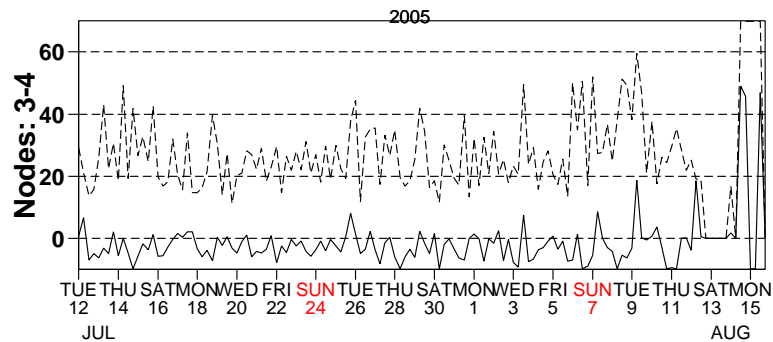
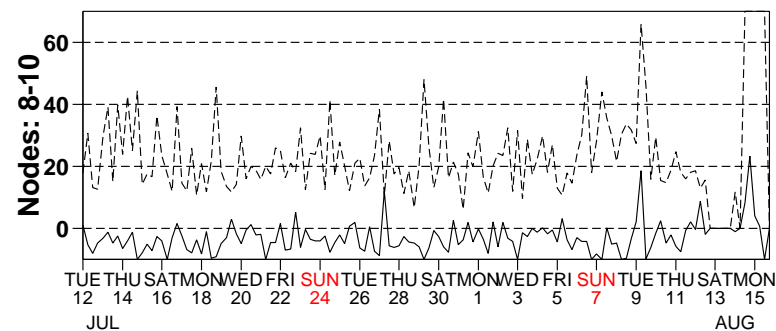
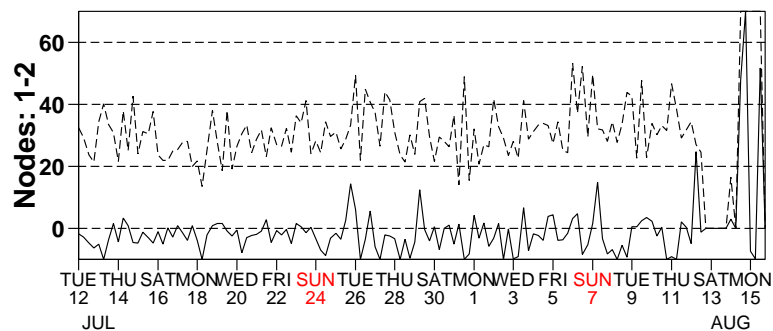
Figure 7

Monitoring of UWI winds versus First Guess for ERS-2

from 2005071200 to 2005081518

(solid) wind direction bias UWI - First Guess over 6h (deg.)

(dashed) wind direction standard deviation UWI - First Guess over 6h (deg.)



2005

2005

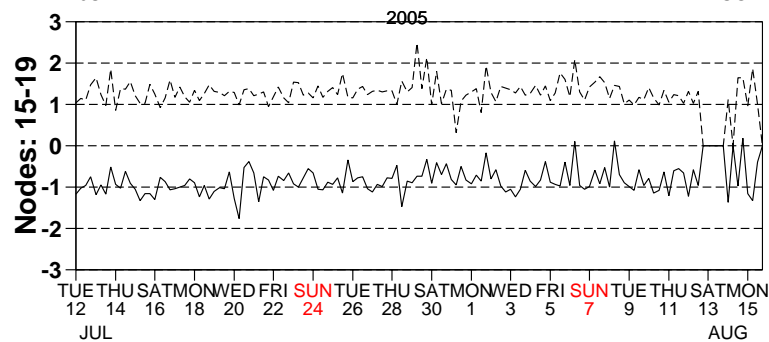
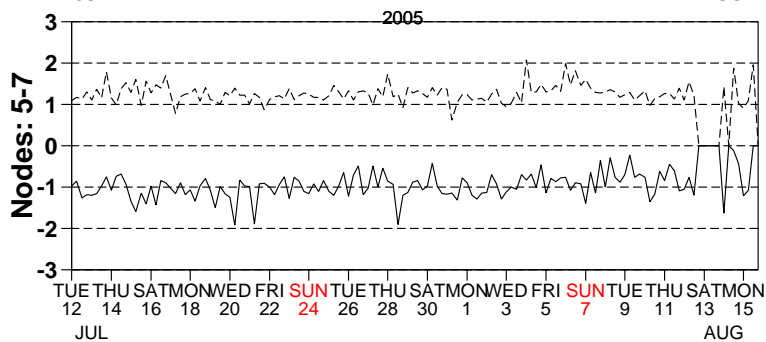
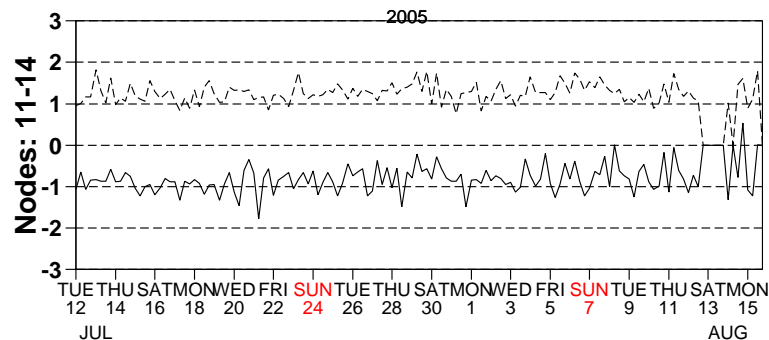
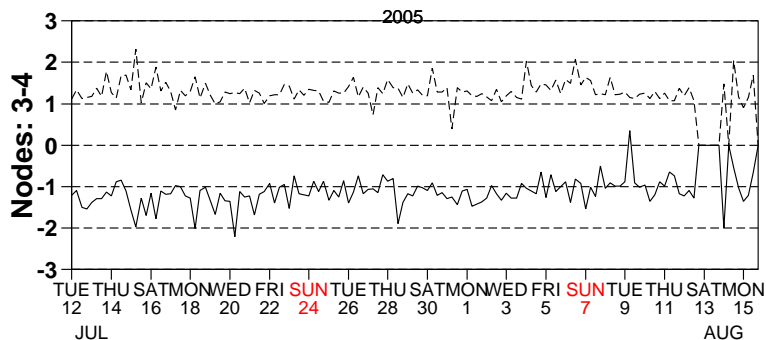
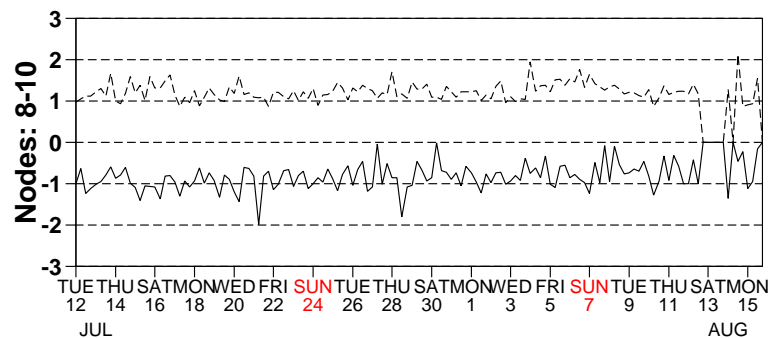
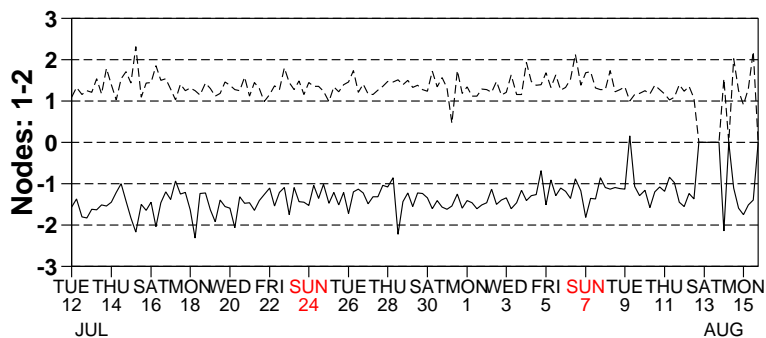
Figure 8

Monitoring of de-aliased CMOD4 winds versus First Guess for ERS-2

from 2005071200 to 2005081518

(solid) wind speed bias CMOD4 - First Guess over 6h (deg.)

(dashed) wind speed standard deviation CMOD4 - First Guess over 6h (deg.)



2005

2005

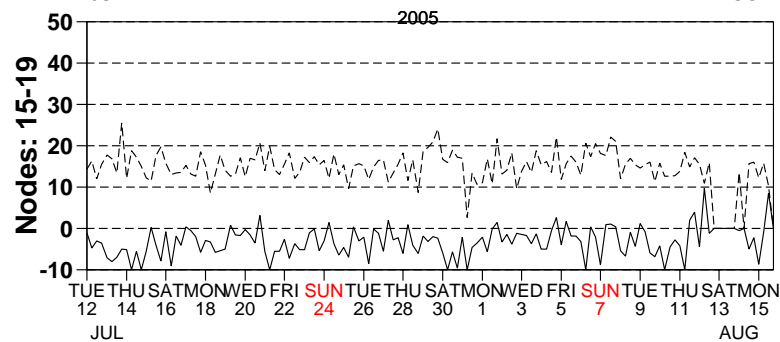
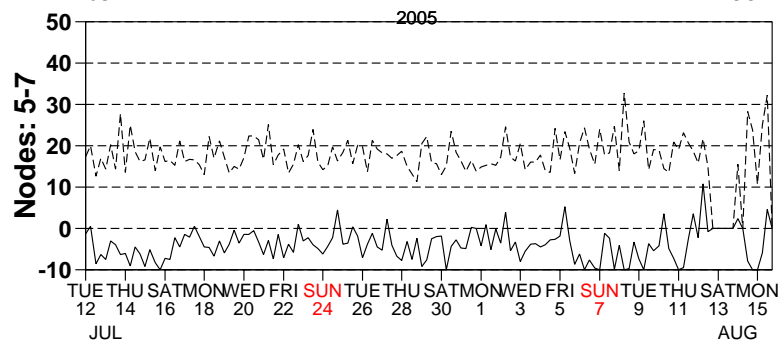
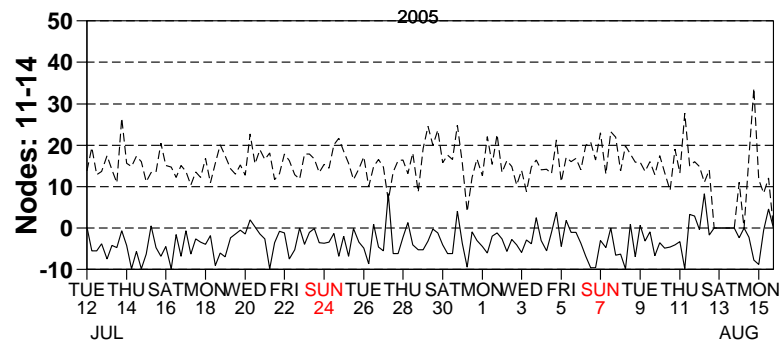
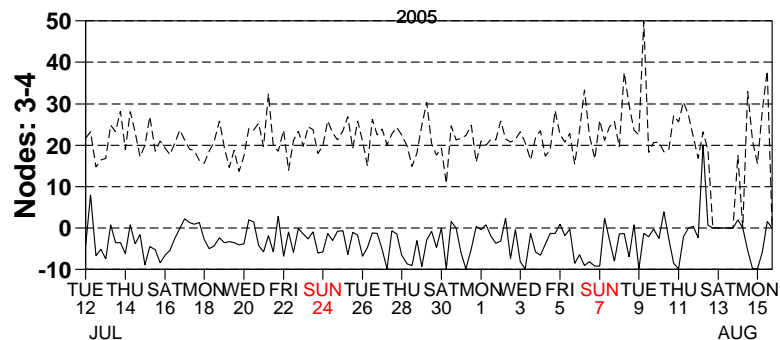
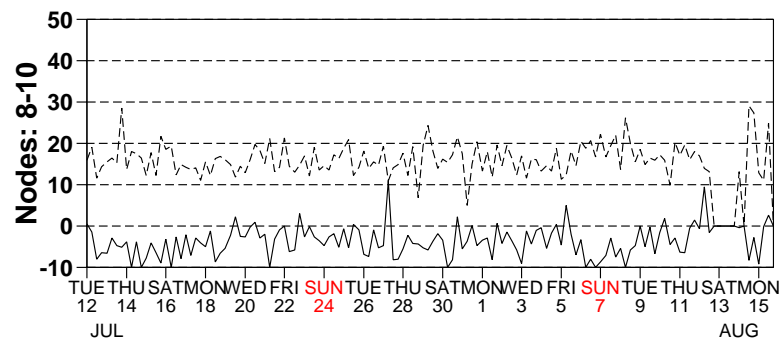
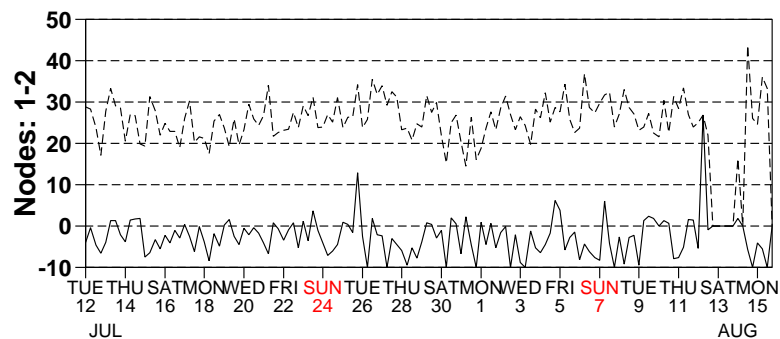
Figure 9

Monitoring of de-aliased CMOD4 winds versus First Guess for ERS-2

from 2005071200 to 2005081518

(solid) wind direction bias CMOD4 - First Guess over 6h (deg.)

(dashed) wind direction standard deviation CMOD4 - First Guess over 6h (deg.)

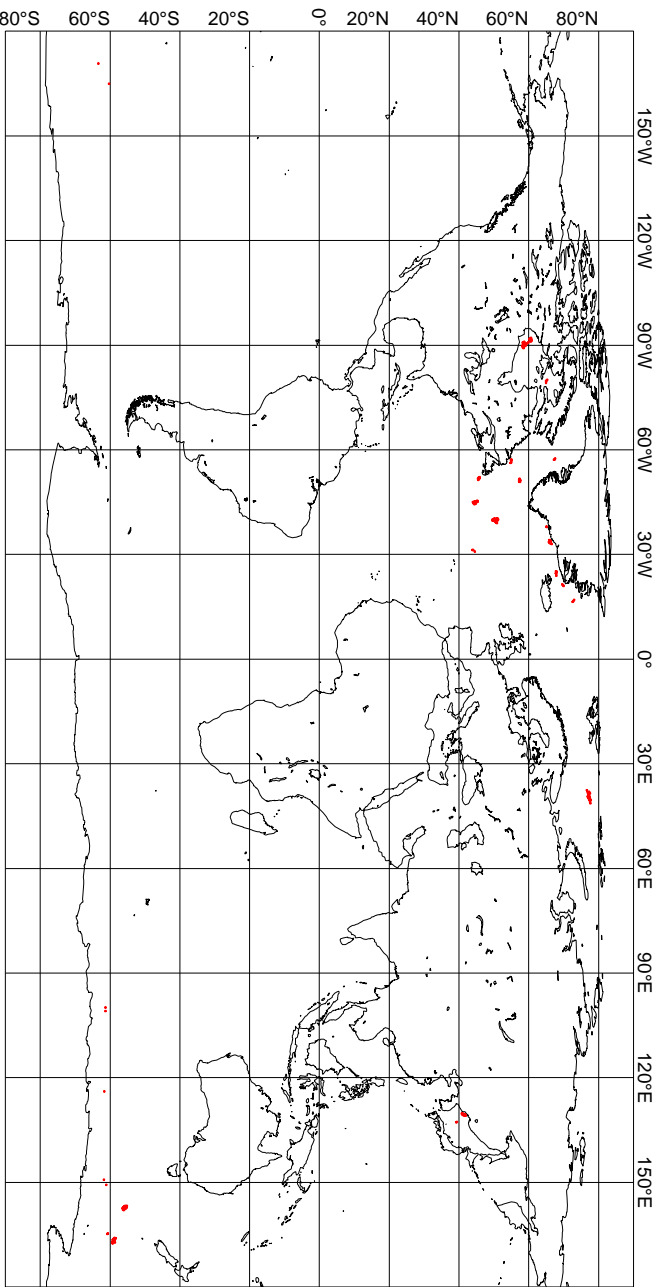


2005

2005

Figure 10

UWI winds more than 8 m/s weaker than FGAT
CYCLE 107, 2005071200 to 2005081518, QC on ESA flags



UWI winds more than 8 m/s stronger than FGAT
CYCLE 107, 2005071200 to 2005081518, QC on ESA flags

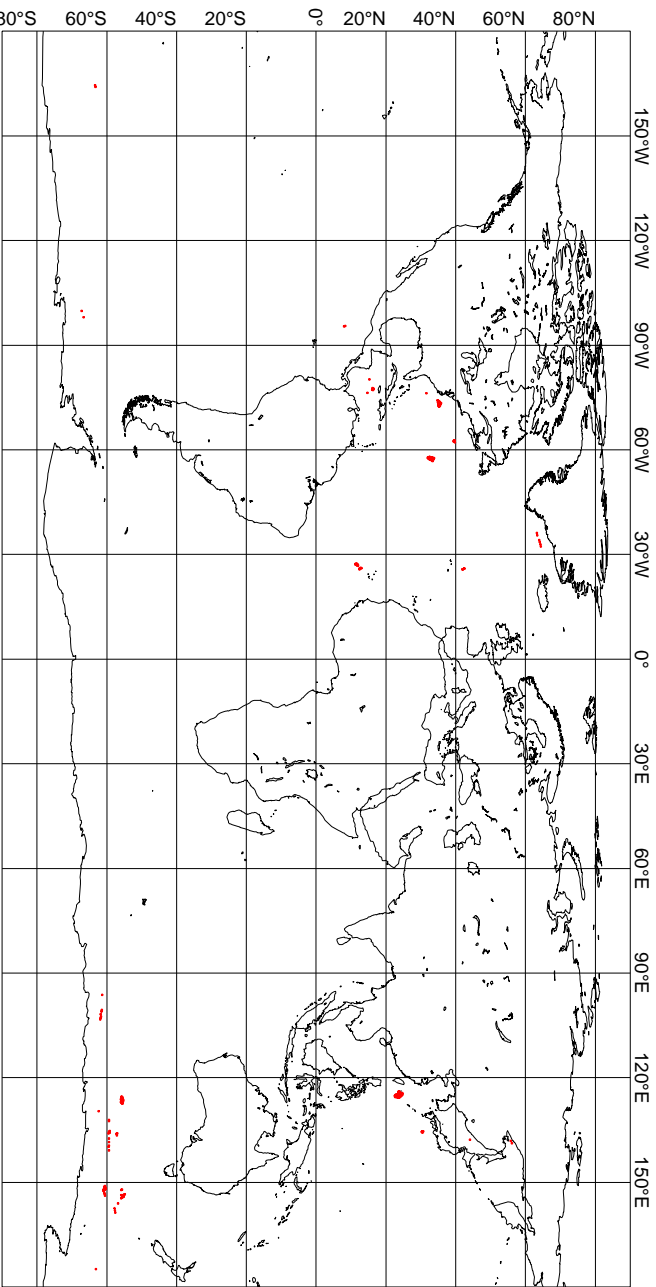
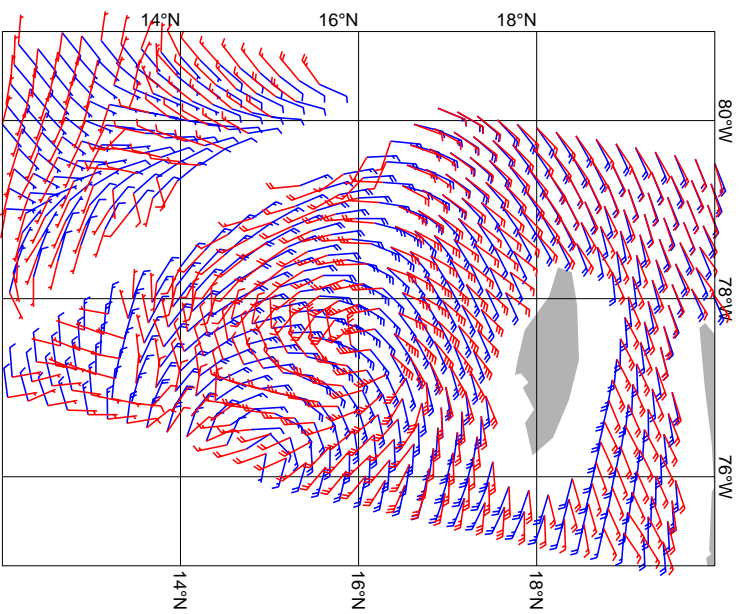


Figure 11

CMOD4 winds (red) versus FGAT winds (blue)
EMILY 20050716 15:33 UTC



CMOD4 winds (red) versus FGAT winds (blue)
MATSA 20050804 02:09 UTC

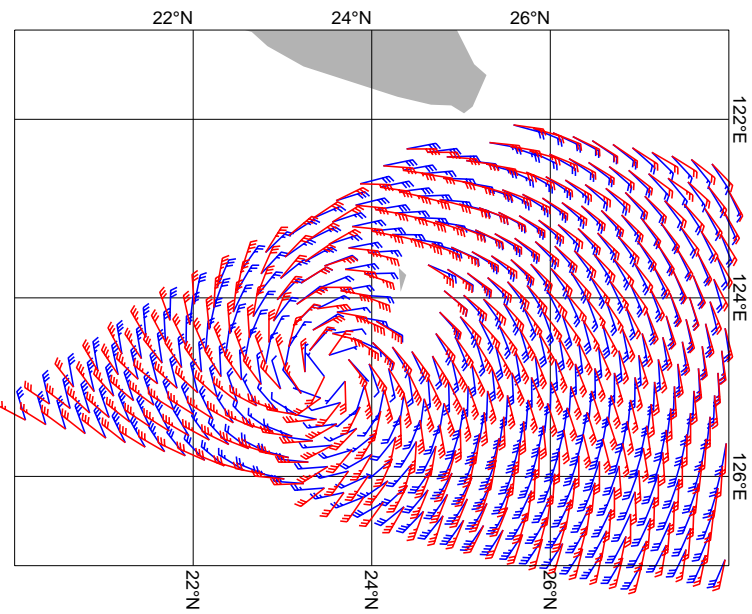


Figure 12

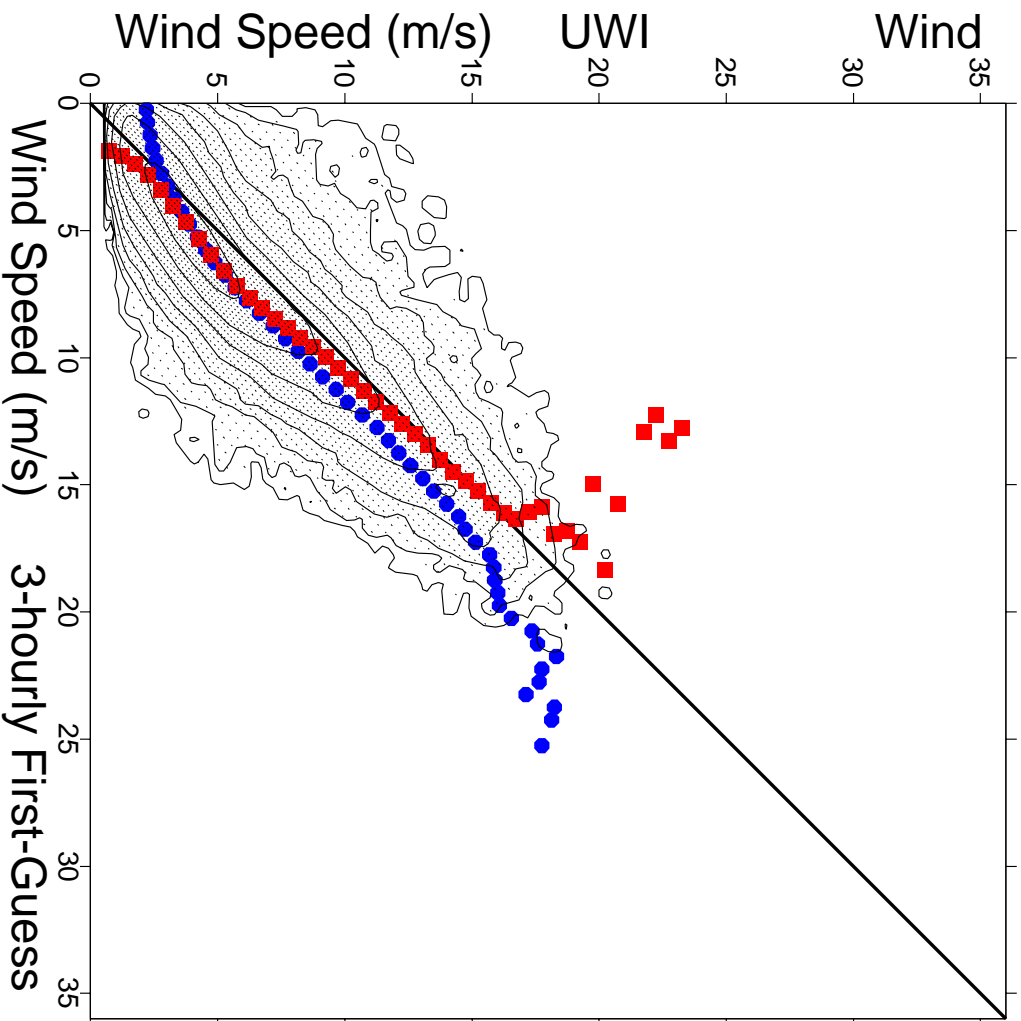


Figure 13

ECMWF 3-hourly First-Guess winds versus UWI winds
from 2005071200 to 2005081518
= 659464 (|f| gt 4.00 m/s), db contour levels, 5 db step, 1st level at 3.2 db
m(y-x)=-3.44 sd(y-x)= 28.80 sdx=107.68 sdy=107.80 pcxy= 0.982

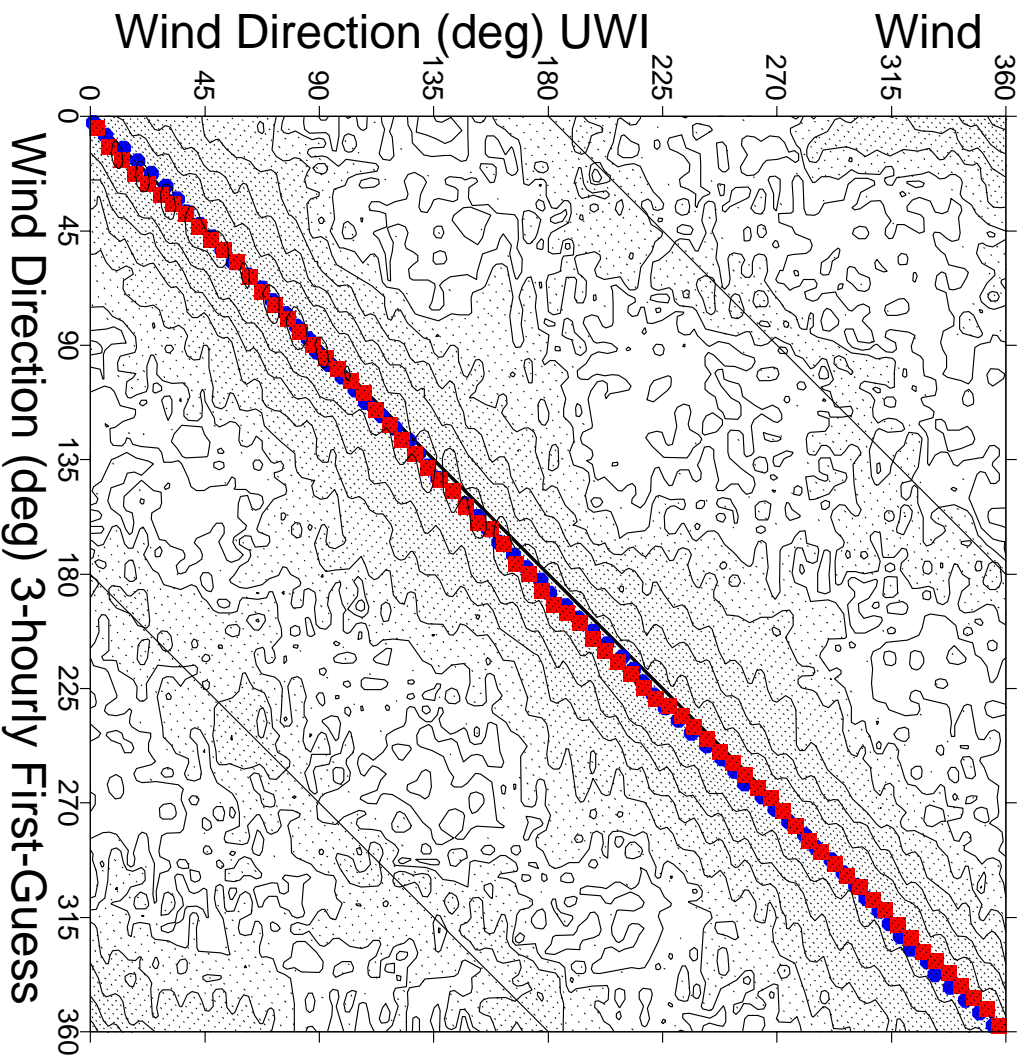


Figure 14

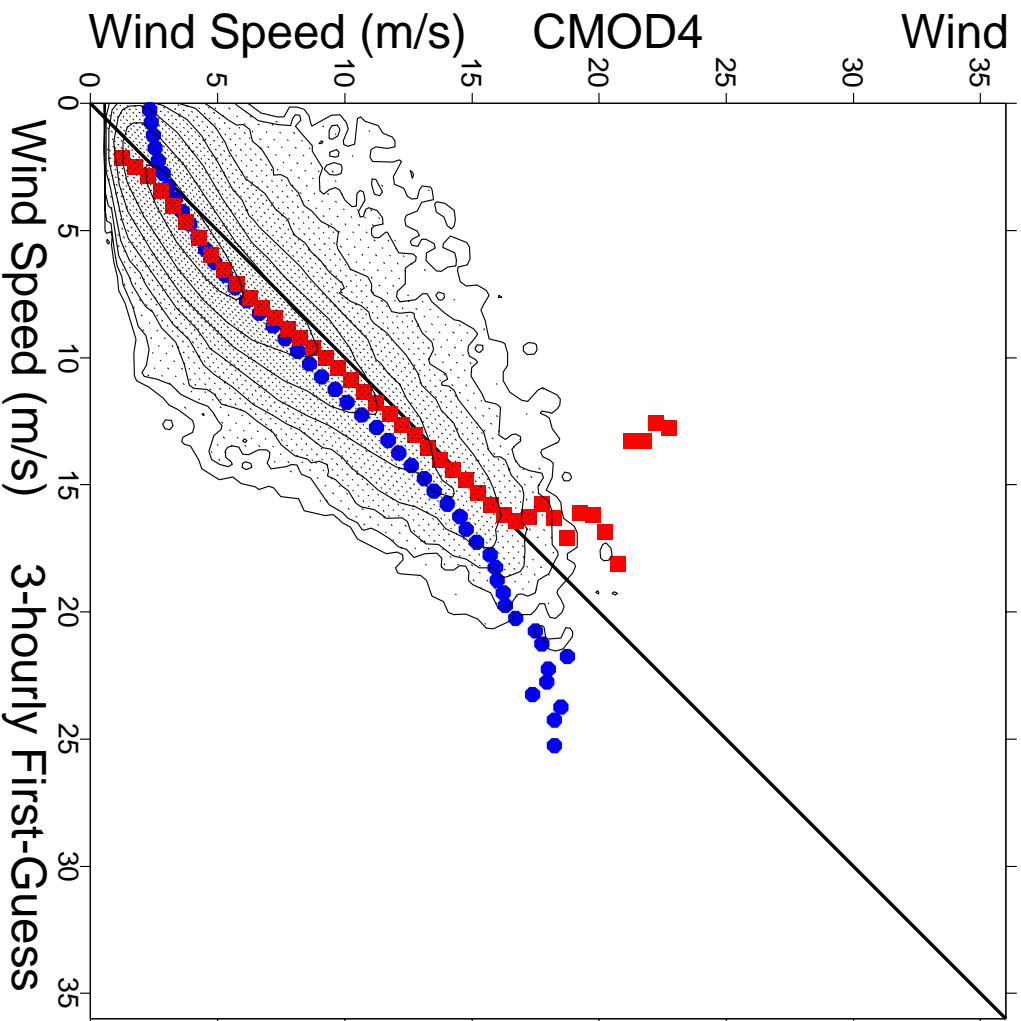


Figure 15

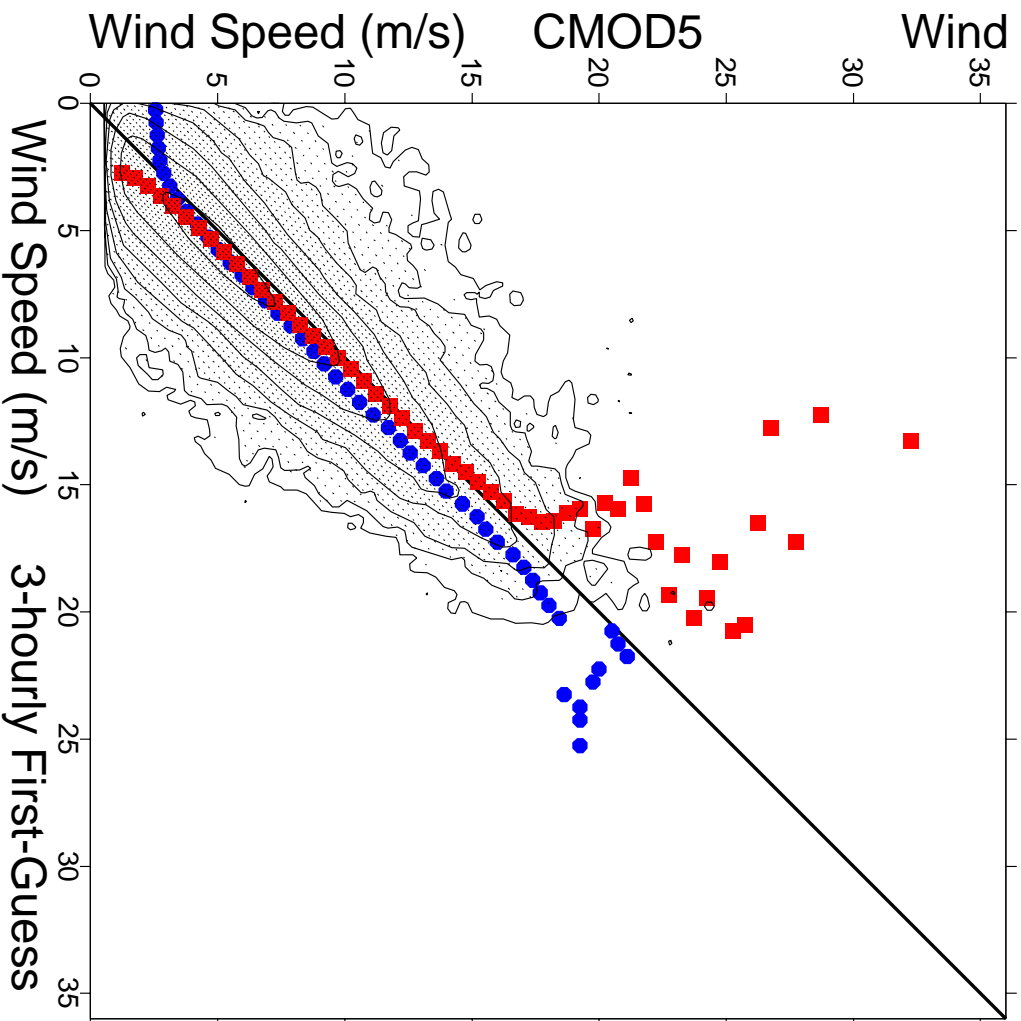
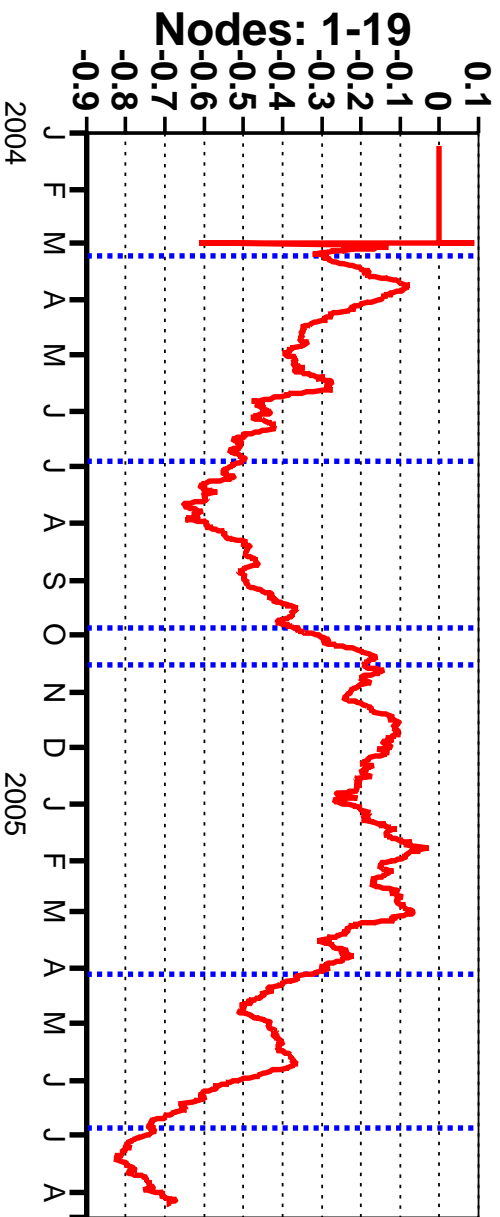


Figure 16

ERS-2 (CMOD5)



QuikSCAT (QSCAT-1)

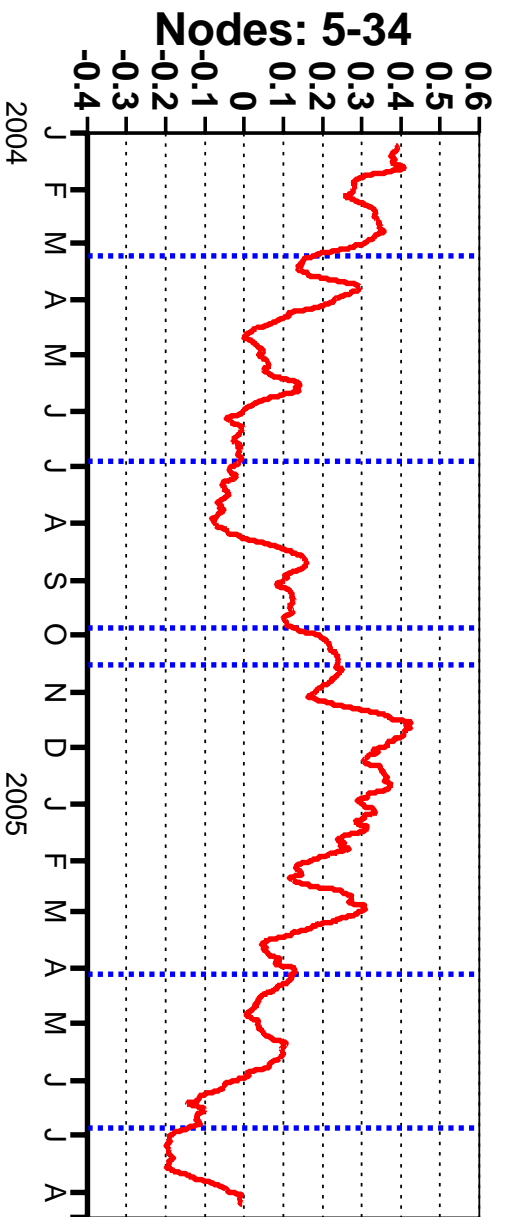


Figure 17